

IMPROVING EARTHQUAKE AND EXPLOSION DISCRIMINATION BY USING LOVE AND RAYLEIGH WAVE MAGNITUDES

Jessie Bonner<sup>1</sup>, Anastasia Stroujkova<sup>1</sup>, and Dale N. Anderson<sup>2</sup>

Weston Geophysical Corporation<sup>1</sup> and Los Alamos National Laboratory<sup>2</sup>

Sponsored by the Air Force Research Laboratory

Award No. FA8718-09-C-0012

Proposal No. BAA09-75

**ABSTRACT**

Since the 1960s, comparing a Rayleigh-wave magnitude,  $M_s$ , to the body-wave magnitude,  $m_b$ , has been a robust tool for the discrimination of earthquakes and explosions (e.g.,  $M_s:m_b$ ). In this article, we apply a Rayleigh-wave formula *as is* to Love waves and examine the possibilities for discrimination using only surface wave magnitudes (e.g.,  $M_s(\text{Rayleigh}):M_s(\text{Love})$ ). To calculate the magnitudes we apply the time-domain magnitude technique called  $M_s(\text{VMAX})$  developed by Russell (2006) to Rayleigh and Love waves from explosions and earthquakes. Our results indicate that for the majority of the earthquakes studied (>75%), the  $M_s(\text{VMAX})$  obtained from Love waves is greater than the estimate from Rayleigh waves. Conversely, 79 of 82 nuclear explosions analyzed (96%) have network-averaged  $M_s(\text{VMAX})$ -Rayleigh equal to or greater than the  $M_s(\text{VMAX})$ -Love.

We use logistic regression to develop an  $M_s(\text{Rayleigh}):M_s(\text{Love})$  discriminant. Cross-validation analysis of the new discriminant correctly identifies 57 of 82 explosions and 246 of 264 earthquakes while misidentifying 22 explosions as earthquakes and 11 earthquakes as explosions. The majority of these misidentified earthquakes are either deep (sub-crustal) earthquakes or the events with normal or thrust focal mechanisms. Further comparative research is planned for  $M_s(\text{Rayleigh}):M_s(\text{Love})$  versus  $M_s:m_b$  using common data.

We expect that  $M_s(\text{Rayleigh}):M_s(\text{Love})$  will contribute significantly to multivariate event identification; however, it does not have the same population separation that has been historically observed for the  $M_s:m_b$  discriminant. Results also suggest that incorporation of Love waves into the analysis requires a re-examination of the period limits currently used for the  $M_s(\text{VMAX})$  technique. While the  $M_s(\text{VMAX})$ -Rayleigh method is currently operational at different data centers using periods between 8 and 25 seconds, we believe that future processing should be extended to 40 seconds, especially in regions with deep earthquakes and complex paths.

## OBJECTIVES

The objective of this research is to apply an  $M_s$  formula, originally developed and applied to Rayleigh waves, to both Love and Rayleigh waves. During the past year, we have applied the method *in the same manner* to both phases for three different earthquake datasets as well as a global dataset of nuclear explosions. We examine whether improved discrimination is possible by combining the Love and Rayleigh wave magnitudes. Finally, we discuss possible methods for improving the analysis (e.g., using longer surface wave periods, different attenuation corrections, etc.) based on results of this study.

## RESEARCH ACCOMPLISHED

### Love Wave Magnitude Estimation

We evaluate applicability of  $M_s(\text{VMAX})$  (Variable-period, MAXimum amplitude surface wave magnitude estimation) to Love waves. The formula for  $M_s(\text{VMAX})$  was developed by Russell (2006) while the measurement technique, which is currently in use at the United States Geological Survey as  $M_s\text{-VX}$ , was developed by Bonner *et al.* (2006).  $M_s(\text{VMAX})$  was developed for Rayleigh waves measured at variable periods between 8 and 25 seconds. It is defined as follows:

$$M_s(\text{VMAX}) = \log(A) + \frac{1}{2} \log(\sin \Delta) + 0.0031 \left(\frac{T_0}{T}\right)^{1.8} \Delta - \log(f_c) - 0.43 - 0.66 \log\left(\frac{T_0}{T}\right), \quad (1)$$

where  $T_0 = 20$  sec is the reference period,  $\Delta$  is the great circle distance in degrees,  $f_c$  is the corner frequency of the filter, the constant (0.43) was obtained for zero-phase, third order Butterworth filter. The second term of Equation 1,  $\frac{1}{2} \log(\sin \Delta)$ , is a correction for the geometrical spreading, the third term,  $0.0031 \left(\frac{T_0}{T}\right)^{1.8} \Delta$ , is a period-dependent attenuation correction and the fifth term,  $-0.66 \log\left(\frac{T_0}{T}\right)$ , is a period-dependent excitation correction.

For this paper, we apply Equation 1 *as is* to Love waves. We use the same processing for the Love waves as Bonner *et al.* (2006) designed for Rayleigh except that for the Love-wave magnitude estimates we filter the transverse components. Examples of Butterworth filtering for Rayleigh and Love waves are shown in Figure 1a, b. The data are filtered at center periods of 8, 9, 10, ... 25 seconds, the maximum amplitude at each period is measured, and Equation 1 is used to form 18 different magnitude estimates for each station (Figure 1b). The magnitude at the period of the maximum amplitude is assigned as the  $M_s(\text{VMAX})$  for a particular station, and combined with other stations to form a network average for an event. For this study, analysts (the first two co-authors) identified all Rayleigh- and Love-wave phases; however, we are currently working on automated methods to identify the phases and measure the amplitudes.

**Earthquakes.** Equation 1 was applied to estimate  $M_s(\text{VMAX})$  for both Rayleigh and Love waves for three separate earthquake datasets (Figure 2). The first dataset (See Figure 2a) included 109 events located in the Middle East with the body wave magnitudes ranging between 3.8 and 6.1. The database samples a variety of different focal mechanisms. The stations used to estimate surface wave magnitudes are distributed throughout Eurasia with distances ranging from approximately 83 to over 10000 km. The data for these stations were obtained from the Incorporated Research Institutions (IRIS) in Seismology Data Management Center (DMC), corrected for the instrument response to displacement in nanometers, and rotated to transverse, radial, and vertical components. The Love wave magnitudes were estimated from the transverse data, while the Rayleigh wave estimates were obtained using the vertical data. The results are plotted in Figure 3a and show that  $M_s(\text{VMAX})$ -Love exceeds or is equal to  $M_s(\text{VMAX})$ -Rayleigh for 82 out of 109 events (75%). The dominant periods of the measurements are approximately 21-22 sec for Rayleigh waves and 25 sec for Love waves. The interstation standard deviation averaged 0.22 magnitude units (m.u.) for both Rayleigh and Love waves.

The second dataset included 31 earthquakes occurring in the Korean Peninsula and surrounding regions (Figure 2c). These events ranged in size between  $3.2 < M_w < 5.1$  with the focal mechanisms being predominantly strike-slip ([http://www.eas.slu.edu/eqc/eqc\\_mt/MECH.KR](http://www.eas.slu.edu/eqc/eqc_mt/MECH.KR), last accessed, April 2011). The distances to the three-component stations recording these events, mainly Korean Meteorological Administration (KMA) and some Global

Seismographic Network (GSN) stations, ranged from 55 km to 1900 km. Similar to the Middle Eastern events, the majority of these events (25 out of 31, or 80%) had  $M_s(\text{VMAX})$ -Love exceeding or equal to the  $M_s(\text{VMAX})$ -Rayleigh, which is expected for a strike-slip mechanism. The dominant periods of the measurements for Rayleigh waves was less than 13 seconds; however, the Love wave magnitudes were uniformly sampled between periods 8 and 20 seconds. The interstation magnitude standard deviation for the Rayleigh and Love waves averaged 0.11 and 0.22 m.u., respectively.

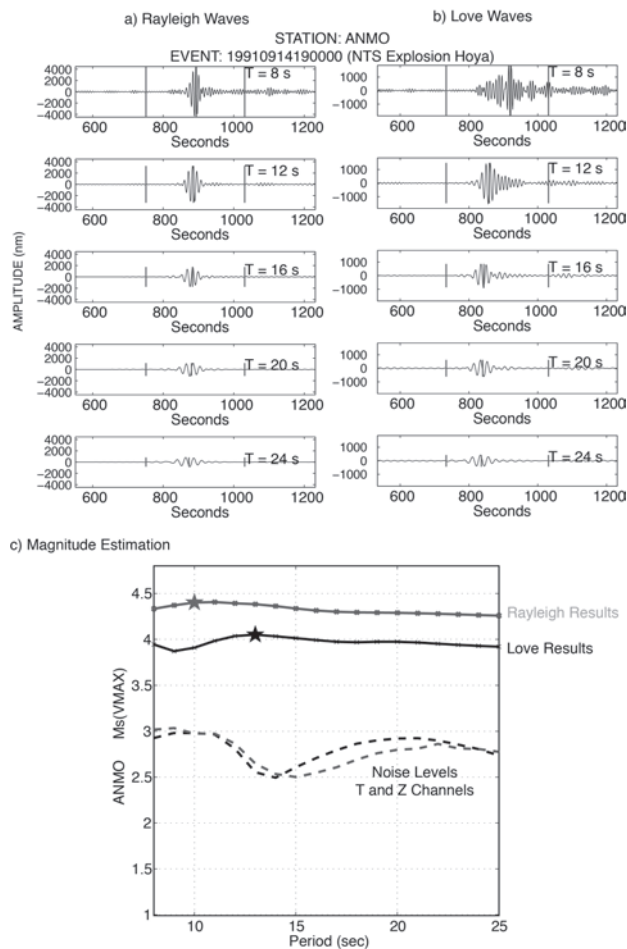
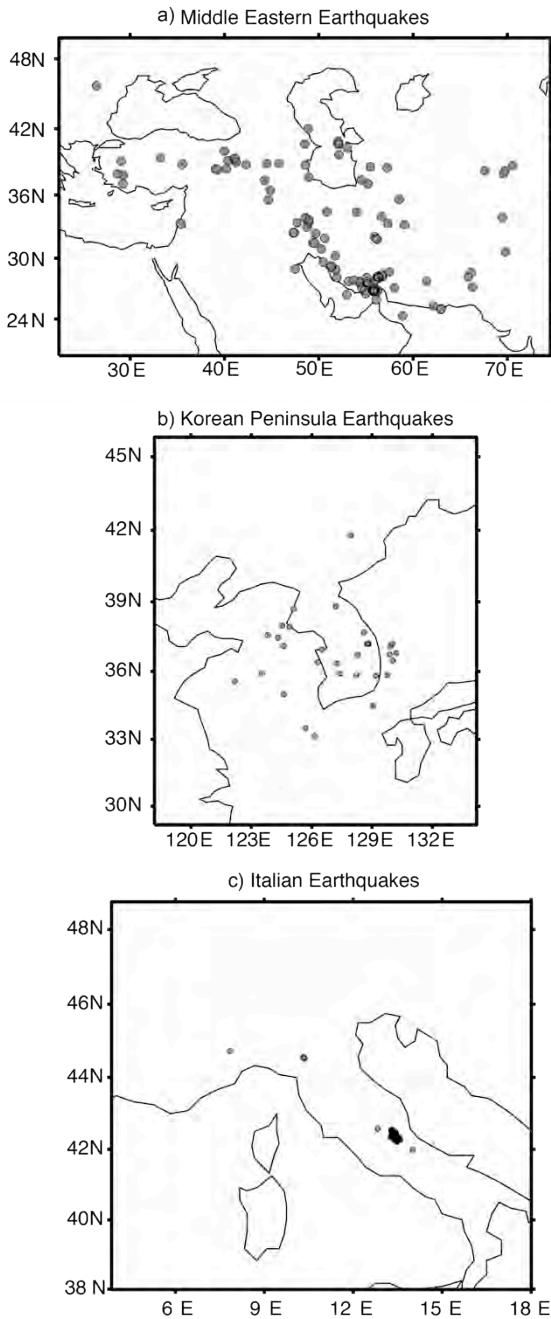
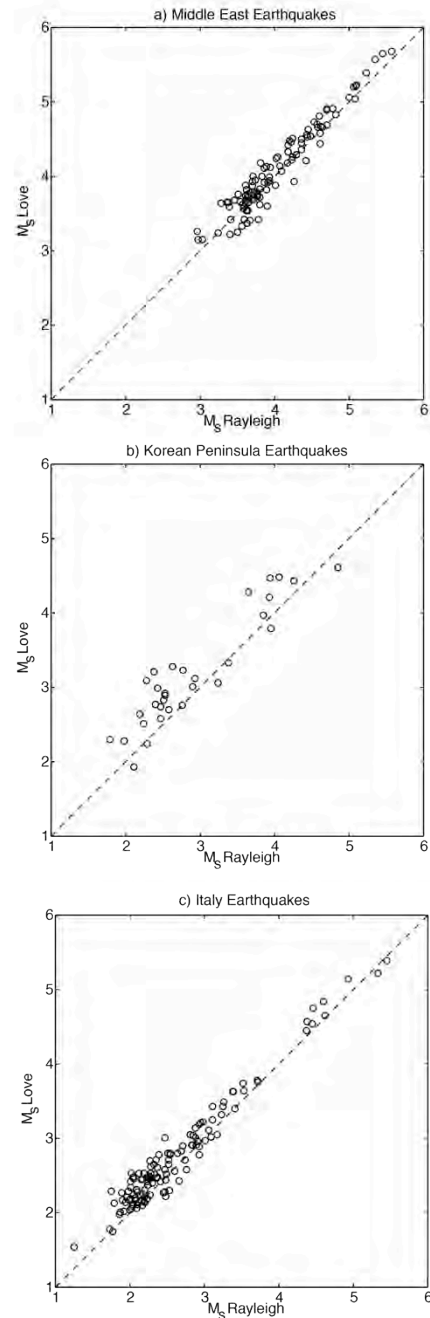


Figure 1. Examples of the  $M_s(\text{VMAX})$  technique applied to a) Rayleigh and b) Love waves from a Nevada Test Site explosion (Hoya). The Butterworth filters are computed at center periods between 8 and 25 seconds (not all filter panels are shown in this figure). The maximum amplitude in each filter band in a Rayleigh and Love wave group velocity window (small vertical lines) is input into Equation 1 and 18 different magnitudes c) are estimated. The magnitude at the period of maximum amplitude (shown as a star) is used as the final  $M_s(\text{VMAX})$  for a station and combined with others for a network average.



**Figure 2.** Map of the seismic events for which  $M_s$  (VMAX)-Love and Rayleigh were estimated in the a) Middle East, b) Korean Peninsula region, and in c) central Italy.



**Figure 3.**  $M_s$ (VMAX)-Love versus  $M_s$  (VMAX)-Rayleigh for earthquakes in the a) Middle East, b) Korean Peninsula region, and in c) central Italy.

The third dataset focused on the damaging L'Aquila earthquake (6 April 2009  $M_w=6.1$ ) and its aftershocks (Figure 2c). We have estimated  $M_s$ (VMAX) for 125 Italian earthquakes with  $2.8 < M_w < 6.1$  using Istituto Nazionale Geofisica e Vulcanologia (INGV) stations at distances ranging from 50 to 414 km. We include these data in our study because the dominant focal mechanism suggests NW/SE trending normal faults ([http://www.eas.slu.edu/eqc/eqc\\_mt/MECH.IT/laquila.png](http://www.eas.slu.edu/eqc/eqc_mt/MECH.IT/laquila.png), last accessed April 2011; Herrmann and Malagnini,

2009). Figure 3c shows that for the majority of these events (100 or 80%)  $M_s(\text{VMAX})$ -Love was on average 0.2 m.u. larger than the  $M_s(\text{VMAX})$ -Rayleigh, which is unexpected for the dip-slip focal mechanisms. The dominant period of the measurements was 8 seconds for Rayleigh waves and between 8 and 12 seconds for the Love waves. The interstation standard deviation for the Rayleigh waves averaged 0.17 m.u., which was slightly lower than for the Love waves (0.20 m.u.).

The percentage of the events with higher  $M_s(\text{VMAX})$ -Love is slightly lower for the Middle East dataset than for Korea and Italy (74% vs. 80%). Possible explanations include deeper events as well as more variety in the focal mechanisms for the Middle Eastern dataset. The interstation standard deviation is slightly higher for the Middle East data, which most likely results from more laterally heterogeneous structure. Another peculiarity of the Middle East dataset is the longer dominant periods at which  $M_s(\text{VMAX})$  is calculated for both Rayleigh and Love waves. Figure 4 shows the histograms of the dominant periods for the Middle East, Korea, and Italy. Excitation due to depth alone cannot explain this period increase, because a similar feature is observed for a nuclear explosion detonated in this study region (EVID 19980528101600). The large number of Love and Rayleigh-wave observations at 25 seconds represents an edge effect associated with the long period limit in the current processing. Increasing this limit to 40 seconds will be discussed later in the paper.

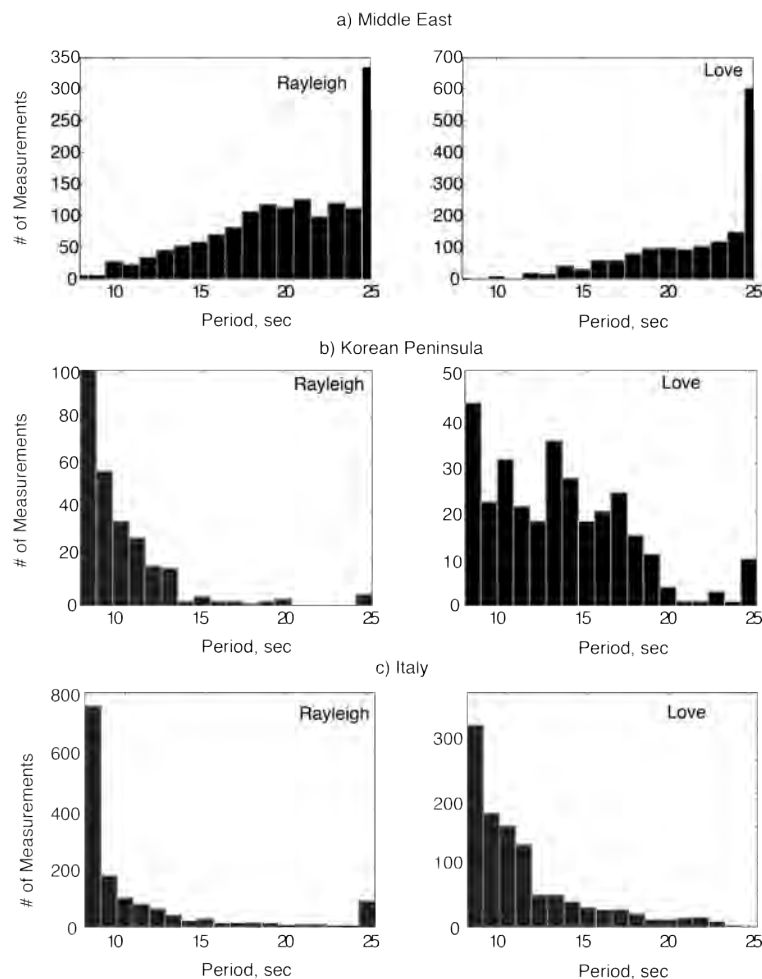


**Figure 4.** Histograms of the periods of maximum amplitudes for Rayleigh and Love waves in the a) Middle East, b) Korean Peninsula region, and in c) central Italy. For the Middle East dataset, varied focal mechanisms, depths, and complex regional-to-teleseismic propagation paths lead to longer period magnitude estimates. For the Korean and Italian datasets, the events are shallow and have shorter, less complex propagation paths leading to more short-period magnitude estimates.

**Explosions.** We have also estimated the  $M_s(\text{VMAX})$  for Rayleigh and Love waves from 82 nuclear explosions at many different test sites (Figure 5). Our working hypothesis was that the Love wave magnitudes should be smaller than the Rayleigh wave estimates for explosions. This was certainly the case for all analyzed events at the Nevada National Security Site (NNSS)—formerly the Nevada Test Site—where  $M_s(\text{VMAX})$ -Rayleigh averaged 0.4 and m.u. larger than  $M_s(\text{VMAX})$ -Love. There were some events with large Love wave magnitudes from the Shagan Test Site; however, the Rayleigh wave magnitudes were on average 0.21 m.u. larger than the Love wave estimates. For 7 Lop Nor explosions the  $M_s(\text{VMAX})$ -Rayleigh are slightly larger than  $M_s(\text{VMAX})$ -Love, except for one anomalous event (EVID 19920521045947 in ES Table 3) which had a Love wave magnitude 0.27 m.u. larger than the Rayleigh magnitude. Our dataset also included the 1998 Pakistan nuclear test, which had a Love wave magnitude slightly larger than the Rayleigh magnitude, and the 1998 Indian nuclear explosion, which had a larger Rayleigh magnitude (by  $\sim 0.2$  m.u.).

We were unable to measure Love waves using openly available data for the 2006 North Korean nuclear explosion ( $M_s(\text{VMAX})$ -Rayleigh=2.9). Based on background noise levels, we conclude the  $M_s(\text{VMAX})$ -Love must have been less than 2.5 (similar conclusion reached by Kohl et al., 2011). For the 2009 event, the Rayleigh  $M_s(\text{VMAX})=3.7$  exceeded the Love  $M_s(\text{VMAX})$  by 0.5 m.u. As mentioned previously, the Korean events had large Rayleigh  $M_s$  estimates compared to  $m_b$ , however, the Love waves magnitudes are much smaller and provide added discrimination information.

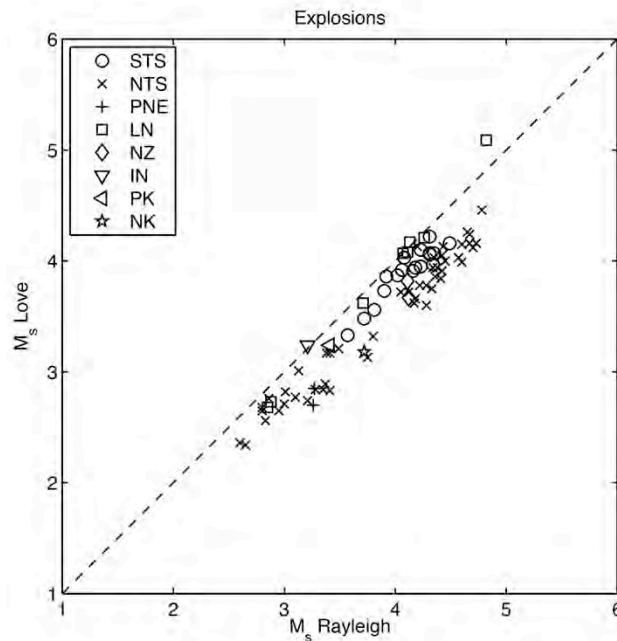


**Figure 5.  $M_s(\text{VMAX})$ -Love versus  $M_s(\text{VMAX})$ -Rayleigh for nuclear explosions.**

### Event Identification with Logistic Regression

The observed differences in the Love and Rayleigh wave magnitudes between earthquakes and explosions led us to an idea that a surface wave discriminant could be developed without incorporation of an  $m_b$ . For regional events,  $m_b(Pn)$  is often difficult to determine, and there may be geophysical structural, data center measurement (e.g., Murphy et al., 1997), and data censoring biases that complicate the  $M_s:m_b$  interpretation. We decided to test for a possible  $M_s:M_s$  discriminant using logistic regression (Press and Wilson, 1978).

Logistic regression models the conditional probability that an event is an explosion given a regression function of event magnitudes  $\underline{x}$ . The calibrated model gives the best linear combination (regression model) of magnitudes (the discriminant) that best agrees with the separation between explosion and earthquake magnitude data. Using the regression model, the Bernoulli probability of an event being an explosion is expressed as

$$\pi(\underline{x}) = \frac{1}{1 + e^{\alpha + \beta' \underline{x}}} \quad (2)$$

For  $n$  observed events, earthquakes and explosions, the likelihood function is defined as the product of these probabilities:

$$\ell(\alpha, \beta) = \prod_{i=1}^n \pi(\underline{x}_i)^{y_i} (1 - \pi(\underline{x}_i))^{1-y_i}, \quad (3)$$

where  $y_i = 1$  if the event is an explosion,  $y_i = 0$  if the event is an earthquake, and  $\underline{x}_i$  is the vector of observed magnitudes for the event. Maximizing  $\ell(\alpha, \beta)$  provides estimates (calibration values) for  $\alpha, \beta$ . For a new event,  $\pi(\underline{x})$  is evaluated with magnitudes  $\underline{x}$  and identification made with this value. For example, if  $\pi(\underline{x}) > 0.55$  the event is identified as explosion, if  $\pi(\underline{x}) < 0.45$  the event is identified as earthquake, and indeterminate otherwise. Figure 6a gives the function  $\pi(\underline{x})$ ,

$$\pi(EX | M_s(Rayleigh), M_s(Love)) = \frac{1}{1 + e^{(4.09 + 12.14 * M_s(Love) - 12.65 * M_s(Rayleigh))}}, \quad (4)$$

using the average jackknife parameter values (see Figures 6b,c,d), and a subset of jackknife event identifications. The indeterminate region is included on plot. We have completed a leave-one-out (jackknife) cross validation analysis (Figures 6 b,c,d) on  $M_s(\text{VMAX})$ -Rayleigh and Love using the decision rule above. The data included 82 explosions and 264 earthquakes. For each jackknife sample, 82+264=346 in total, calibration values for  $\alpha, \beta$  were computed using maximum likelihood estimation. These parameter values were then used to identify the hold-out event by evaluating  $\pi(\underline{x})$  and applying the decision criteria above. The performance of the cross validation analysis is given in Table 1. From Figure 6e, we note that the absolute values of the slopes for earthquakes and explosions are statistically different.

**Table 1. Cross Validation Identification Performance with  $M_s$  Rayleigh and Love Magnitudes.**

	EX	EQ	I	Total
EX	57	22	3	82
EQ	11	246	7	264

The cross-validation analysis of the proposed  $M_s:M_s$  discriminant correctly identifies 57 of 82 explosions and 246 of 264 earthquakes. The analysis misidentifies 22 explosions as earthquakes and 11 earthquakes as explosions. These results show that there is discrimination information in an  $M_s(\text{Rayleigh}):M_s(\text{Love})$  discriminant. Further comparative research is planned for  $M_s(\text{Rayleigh}):M_s(\text{Love})$  versus  $M_s:m_b$  using common data. We fully expect that  $M_s(\text{Rayleigh}):M_s(\text{Love})$  will contribute significantly to multivariate event identification. Results from this study do suggest that a  $M_s\text{-Love}:m_b$  discriminant might be more robust than  $M_s\text{-Rayleigh}:m_b$  due to the typically larger  $M_s\text{-Love}$  magnitudes for earthquakes and smaller values for explosions. However, the smaller  $M_s\text{-Love}$  estimates for explosions, while great for discrimination, are costly in terms of detection. Bonner *et al.* (2006) determined for  $M_s(\text{VMAX})$ -Rayleigh to be measured at the NNSS, the  $m_b$  must be 3.6 or greater; thus the event body-wave magnitude for  $M_s(\text{VMAX})$ -Love application would increase to greater than 4.0.

**Possible Improvements to Love Wave Magnitude Estimation**

The objective of this study was to evaluate Equation 1 *as is* for Love waves from both earthquakes and explosions; however, we do note that some terms in Equation 1 could change for Love waves. In the next few paragraphs, we

discuss possible changes for future application of this technique, including the source excitation and attenuation corrections and the need to incorporate additional periods into the analysis.

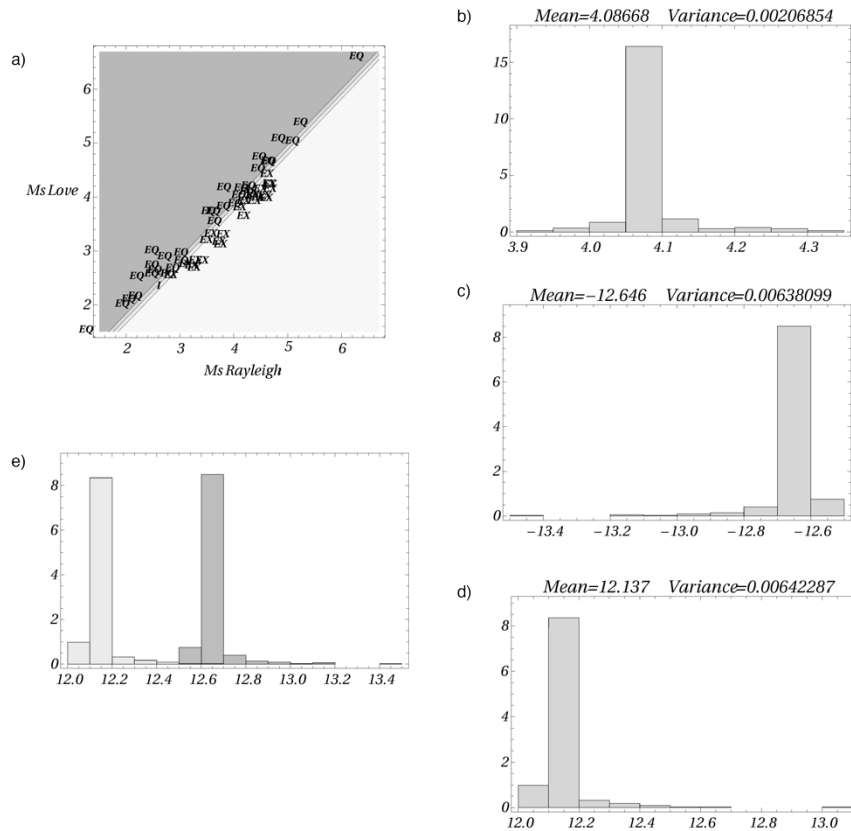


**Figure 6.** Logistic regression results for a possible  $M_s(\text{Rayleigh}):M_s(\text{Love})$  discriminant. a)  $\pi(\underline{x})$  using the average of jackknife parameter values. b) Jackknife  $\alpha$  estimates. c) Jackknife estimates of Rayleigh slopes. d) Jackknife estimates of Love slopes. e) Histograms of the absolute value jackknife slopes  $\underline{\beta}$ . Rayleigh jackknife slopes are gray and Love jackknife slopes are light gray.

**Excitation Correction.** The “source excitation” correction  $-0.66 \log \left( \frac{T_0}{T} \right)$  in Equation 1 is slightly misleading, because the correction is actually for the effects of the source depth and structure at the source rather than for the actual source spectra. A shallow explosion will generate large amplitude, short-period ( $< 20$  secs) surface waves (and magnitudes) relative to  $T_0=20$  seconds, where most historical measurements have been made, and thus must be reduced in order to improve explosion and earthquake discrimination and provide better agreements with historical magnitude scales. This correction accomplishes this need and is determined empirically by modeling Rayleigh waves generated by 1 km deep explosions in a variety of different velocity structures (Bonner et al., 2006).

Since Love waves are not generated by isotropic explosions, we determined a corresponding correction for the Love waves using a 1 km deep double-couple earthquake for different velocity structures. A similar expression for the Love wave source excitation is  $-0.45 \log \left( \frac{T_0}{T} \right)$  which is similar to the one incorporated into the Russell (2006) equation. For future examination, a more rigorous and model-dependent approach to this correction, such as discussed in Stevens and McLaughlin (2001) and Stevens et al. (2007), could lead to improved results.

**Attenuation Correction.** To investigate the applicability of the attenuation correction in Equation 1 to Love waves, we first subtracted the correction  $\left[0.0031 \left(\frac{r_0}{T}\right)^{1.8} \Delta\right]$  from our estimated  $M_s(\text{VMAX})$  then computed new corrections in the form  $[\alpha\Delta]$  for both Rayleigh and Love waves. The attenuation coefficients calculated as a result are  $\alpha = 0.0037$  for the Rayleigh and  $\alpha = 0.0042$  for the Love waves, compared to 0.0031 in the original formula. Application of the new attenuation corrections improves the residuals for the events used in the inversion; however, it did not improve the RMS residuals for the entire Middle Eastern data set. Future application of this technique could possibly incorporate 2D or 3D attenuation models for Love and Rayleigh waves (Levshin et al., 2007; Stevens et al., 2006, 2007).

**Period Limitations.**  $M_s(\text{VMAX})$  was originally designed for Rayleigh waves in the period range between 8 and 25 sec. However, for some focal mechanisms, deep events, and complex paths, the maximum of the surface wave amplitudes may be achieved at longer periods. Limiting the period range to 25 seconds for the Middle East data (Figure 4) results in numerous measurements that are “pegged” at the upper limit of 25 sec. Increasing the upper limit from 25 sec to 40 sec results in higher magnitude measurements (Figure 7; compare to Figure 4a), which provides a more reliable estimate of source size and slightly lower standard error for both Rayleigh (e.g., 0.22 m.u. to 0.21 m.u.) and Love waves (0.22 m.u. to 0.20 m.u.).

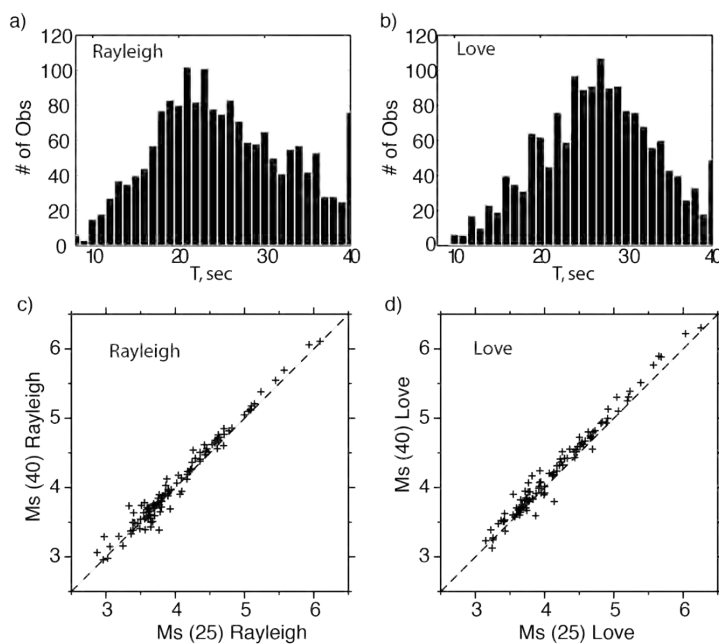


**Figure 7. Results of extending to analysis periods for  $M_s(\text{VMAX})$  to 40 secs for a) Rayleigh and b) Love waves in the Middle East. The estimated c) Rayleigh and d) Love wave magnitudes are often increased by extending the analysis period to 40 secs.**

## CONCLUSIONS AND RECOMMENDATIONS

We conclude that estimating a Love wave magnitude, using the same formula and methods employed for Rayleigh waves, can lead to improved earthquake and explosion discrimination due to the fact that the earthquakes typically have a larger  $M_s$ -Love, while explosions normally exhibit a smaller  $M_s$ -Love when compared to the  $M_s$ -Rayleigh. We conclude that an  $M_s:M_s$  discriminant is possible; however, it does not have the same population separation that has been historically observed for the  $M_s:m_b$  discriminant. Results also suggest that incorporation of Love waves into the analysis requires a re-examination of the period limits currently used for the  $M_s(\text{VMAX})$  technique. While the  $M_s(\text{VMAX})$ -Rayleigh method is currently operational at different data centers using periods between 8 and 25 seconds, we do believe that future processing should be extended to 40 seconds, especially in regions with deep earthquakes and complex paths.

## ACKNOWLEDGEMENTS

We wish to thank Drs. David Russell, Robert Herrmann, and Harley Benz for their assistance with this collaboration and research. We thank Drs. Jack Murphy, Eli Baker, Paul Richards, and Jeff Stevens for suggestions regarding datasets and future directions. We thank Dr. Anton Dainty for his dedicated service to the Bulletin of the Seismological Society as an Associate Editor for nuclear explosion monitoring papers. We thank Mr. Jim Lewkowicz for his continued support and thoughtfulness. And, we thank Dr. Robert Herrmann for valuable information gleaned from personal communications.

## REFERENCES

- Bonner, J. L., D. Russell, D. Harkrider, D. Reiter, and R. Herrmann (2006). Development of a Time-Domain, Variable-Period Surface Wave Magnitude Measurement Procedure for Application at Regional and Teleseismic Distances, Part II: Application and  $M_s$ — $m_b$  Performance. *Bull. Seismol. Soc. Am.* 96, 678–696
- Herrmann, R. B. And L. Malagnini (2009). Fault dynamics of the April 6, 2009 L'Aquila Italy earthquake sequence (draft).
- Levshin, A., X. Yang, M. Ritzwoller, M. Barmin, and A. Lowry (2007). Toward a Rayleigh wave attenuation model for Central Asia. in *Proceedings of the 28th Seismic Research Review: Ground-Based Nuclear Explosion Monitoring Technologies*, LA-UR-06-5471, Vol. 1, pp. 82–92.
- Murphy, J. R., B. W. Barker, and M. E. Marshall (1997). Event screening at the IDC using the  $M_s/m_b$  discriminant. Maxwell Technologies Final Report. 23 p.
- Kohl, B., J. R., Murphy, J. Stevens, and T. J. Bennett (2011). Exploitation of the IMS and other data for a comprehensive advanced analysis of the North Korean nuclear tests, Proceedings of the 2011 Science and Technology Meeting of the CTBTO. 8-10 June 2011. Hofburg Palace, Vienna.
- Press, S. J. and S. Wilson (1978). Choosing Between Logistic Regression and Discriminant Analysis. *J. Am. Stats. Assoc.*, 73: 699–705.
- Russell, D. R. (2006). Development of a time-domain, variable-period surface wave magnitude measurement procedure for application at regional and teleseismic distances. Part I—Theory. *Bull. Seism. Soc. Am.* 96: 665–677.
- Stevens, J. L. and K.L. McLaughlin (2001). Optimization of surface wave identification and measurement, in *Monitoring the Comprehensive Nuclear Test Ban Treaty: Surface Waves*, eds. Levshin, A. and M.H. Ritzwoller, *Pure Appl. Geophys.*, 158: 1547–1582.
- Stevens, J., J. Given, G. Baker, and H. Xu. (2006). Development of surface wave dispersion and attenuation maps and improved methods for measuring surface waves, in *Proceedings of the 28<sup>th</sup> Seismic Research Review: Ground-Based Nuclear Explosion Monitoring Technologies*, LA-UR-06-5471, Vol. 1, pp. 273–281.
- Stevens, J., J. Given, H. Xu, and G. Baker (2007). Development of surface wave dispersion and attenuation maps and improved methods for measuring surface waves, in *Proceedings of the 29<sup>th</sup> Seismic Research Review: Ground-Based Nuclear Explosion Monitoring Technologies*, LA-UR-07-5613, Vol. 1, pp. 282–291.